

Manganese(II), Nickel(II), and Palladium(II) Complexes of a Terpyridine-Like Ligand Containing a Sulfur Linkage, and an Analogous NCN Pincer Palladium(II) Complex: Synthesis, Characterization, and Pd-Catalyzed Reactions

Masakazu Hirotsu,* Yuhei Tsukahara, and Isamu Kinoshita

Department of Material Science, Graduate School of Science, Osaka City University, Sumiyoshi-ku, Osaka 558-8585

Received March 15, 2010; E-mail: mhiro@sci.osaka-cu.ac.jp

Coordination properties of new polypyridines containing a single sulfur linkage, 6-(2″-pyridylthio)-2,2′-bipyridine (L^1) and 1-(2′-pyridyl)-3-(2″-pyridylthio)benzene (HL^2), are described. The manganese(II) and nickel(II) complexes of the terpyridine-like ligand L^1, $[MnCl_2(L^1)]$ (**1**), $[NiCl(\mu\text{-}Cl)(L^1)]_2$ (**2**), and $[Ni(L^1)_2](SbF_6)_2$ (**3**), were prepared and characterized by UV–vis spectroscopy and X-ray crystallography. The palladium(II) complex $[PdCl(L^1)]Cl$ (**4**) was synthesized from L^1 and $Li_2[PdCl_4]$ at room temperature, while the corresponding NCN pincer complex of L^2, $[PdCl(L^2)]$ (**5**), was synthesized in DMSO at 150 °C by cyclopalladation of the ligand precursor HL^2. The crystal structures of **4** and **5** revealed similar coordination geometries around Pd except for the longer Pd–Cl distance in **5**, which is induced by the strong trans influence of the Pd–C bonding. The NMR spectra of **4** showed partial dissociation of L^1 in DMSO-d_6, which was not observed for L^2 in **5**. Catalytic activities of **4** and **5** for the Mizoroki–Heck reaction were investigated, and the lower activity of **5** can be related to the strong σ-donating character of L^2.

Planar tridentate ligands based on 2,2′:6′,2″-terpyridine (terpy) have been widely used for transition-metal complexes incorporated in supramolecular architecture and multicomponent reaction systems.[1,2] The special attention of terpyridine metal complexes are their outstanding photophysical properties.[3,4] A major advantage of terpyridine relies on the inherent stability of its complexes, which is due to the strong coordinating ability and dynamic chelate effect. Mono- and bis-complexes of terpyridines are easily prepared under stoichiometric reaction conditions. Therefore various photoinduced electron- or energy-transfer systems have been developed using functionalized terpyridine derivatives.[5]

Recent studies showed that transition-metal complexes of terpyridines are useful as catalysts. For example, a di-μ-oxo manganese complex of terpyridine catalyzes the conversion of sodium hypochlorite to molecular oxygen.[6] Catalytic cross-coupling reactions were reported for terpyridine nickel complexes.[7,8] Enantioselective cyclopropanations were carried out using copper or rhodium complexes of chiral terpyridines.[9,10] To refine the steric and electronic character of the metal center in terpyridine complexes, the three pyridine rings of terpyridine were functionalized without changing its backbone. On the other hand, pyridine-based pincer complexes containing a metal–carbon bond were used in catalysis, and the palladium(II) complexes with two six-membered metallacycles showed high catalytic performance in the Mizoroki–Heck reaction compared to the five-membered analogs.[11,12] The modification of the chelate rings size is also important for the development of new catalytic systems.

In this paper we report a new class of polypyridines containing a single sulfur linkage: 6-(2″-pyridylthio)-2,2′-bipyridine (L^1) and 1-(2′-pyridyl)-3-(2″-pyridylthio)benzene (HL^2) (Chart 1). The coordination properties of the *N*,*N*,*N*-tridentate ligand L^1 were investigated using manganese(II), nickel(II), or palladium(II) ion. The cyclopalladation of the ligand precursor HL^2 provided a palladium(II) complex with a N–C–N sequence of donor atoms. The palladium(II) complexes of L^1 and L^2 were compared in structure, solution behavior, and catalytic activity in the Mizoroki–Heck reaction.

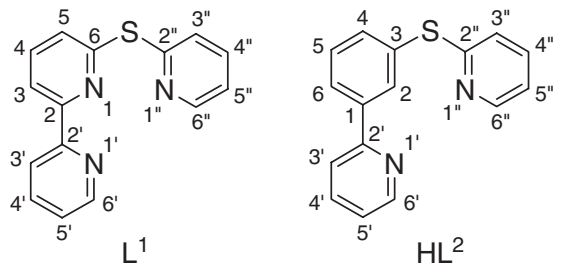

Chart 1.

Results and Discussion

Synthesis of Ligands. The pyridine-based tridentate ligand L^1 was synthesized by the reaction of 6-bromo-2,2′-bipyridine with pyridine-2-thiol in 1,2-propanediol (Scheme 1). Purification by silica gel column chromatography gave a pale yellow oil of L^1 in 81% yield.

The ligand precursor HL^2 for the NCN ligand was obtained from 1,3-dibromobenzene in three steps according to Scheme 2. Treatment of 1,3-dibromobenzene with pyridine-2-thiol gave the monosubstituted product 1-bromo-3-(2′-pyridylthio)benzene in 31% yield after purification by column

Published on the web August 21, 2010; doi:10.1246/bcsj.20100076

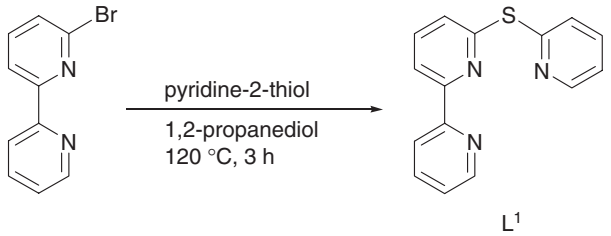

Scheme 1. Synthesis of the *N*,*N*,*N*-tridentate ligand L^1.

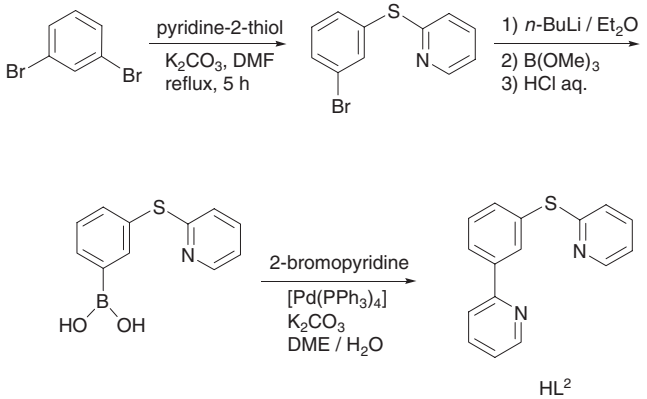

Scheme 2. Synthesis of a precursor for the *N*,*C*,*N*-tridentate ligand L^2.

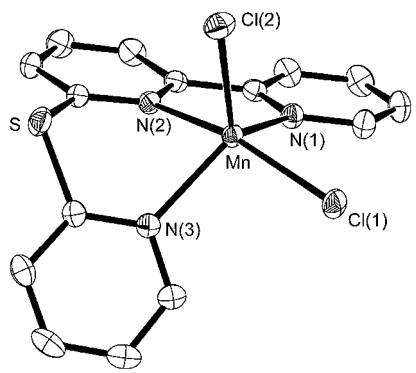

Figure 1. ORTEP drawing of **1** with thermal ellipsoids at the 50% probability level. Hydrogen atoms are omitted for clarity.

chromatography. Bromine–lithium exchange with *n*-butyllithium followed by the reaction with trimethyl borate and then hydrolysis resulted in the formation of 3-(2′-pyridylthio)phenylboronic acid in 65% yield. The palladium-catalyzed cross-coupling reaction of the boronic acid with 2-bromopyridine afforded HL^2 as a pale yellow solid in 85% yield.

Synthesis and Structure of Manganese(II) Complex 1. The manganese(II) complex $[MnCl_2(L^1)]$ (**1**) was prepared by the reaction of $MnCl_2 \cdot 4H_2O$ with an equimolar amount of L^1 in ethanol. Vapor diffusion of diethyl ether into a methanol solution of **1** gave yellow crystals, from which the crystal structure was obtained (Figure 1). The manganese ion is surrounded by three N donors of an L^1 ligand and two chloride ions to form a five-coordinate structure. The bond lengths and angles around Mn are listed in Table 1. The two largest angles

Table 1. Selected Bond Lengths/Å and Angles/° for **1**

Mn–N(1)	2.2440(12)	Mn–Cl(1)	2.3949(4)
Mn–N(2)	2.2756(12)	Mn–Cl(2)	2.3471(4)
Mn–N(3)	2.2414(12)		
Cl(1)–Mn–Cl(2)	105.953(13)	Cl(2)–Mn–N(2)	94.88(3)
Cl(1)–Mn–N(1)	93.62(3)	Cl(2)–Mn–N(3)	116.84(3)
Cl(1)–Mn–N(2)	158.13(3)	N(1)–Mn–N(2)	71.97(4)
Cl(1)–Mn–N(3)	94.72(3)	N(1)–Mn–N(3)	125.58(4)
Cl(2)–Mn–N(1)	112.06(3)	N(2)–Mn–N(3)	81.40(4)
C(10)–S–C(11)	101.43(6)		

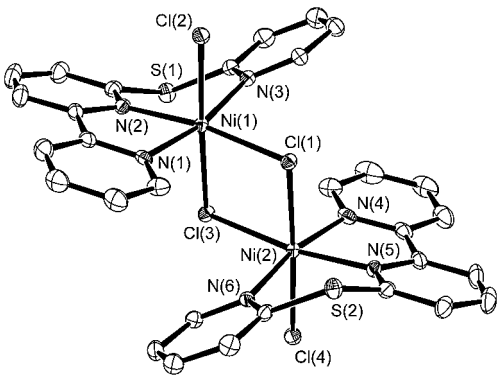

Figure 2. ORTEP drawing of **2** with thermal ellipsoids at the 50% probability level. Hydrogen atoms are omitted for clarity.

are 158.13(3)° of Cl(1)–Mn–N(2) and 125.58(4)° of N(1)–Mn–N(3). The structural index parameter τ for **1** becomes 0.54, where $\tau = (\beta - \alpha)/60$ (α and β are the two largest bond angles around the metal ion, $\beta > \alpha$).[13] This indicates that the geometry around Mn is between trigonal bipyramidal and square pyramidal. A modified index parameter, χ, has been proposed to describe the trigonality of five-coordinate complexes, where $\chi = (\beta + \gamma + \delta - 2\alpha)/180$ (γ and δ represent the remaining bond angles around the metal ion without the donor atoms defining β).[14] The χ value for **1** is 0.75, which suggests that the geometry around Mn in **1** is better described as a distorted trigonal bipyramid with the two apical positions occupied by Cl(1) and N(2). The Mn–Cl(1) and Mn–N(2) bonds are slightly longer than Mn–Cl(2) and Mn–N(terminal), respectively. The corresponding manganese(II) complex of terpyridine, $[MnCl_2(terpy)]$, was reported as a distorted square pyramid with the NNNCl basal plane: the τ and χ values are 0.04 and 0.34, respectively.[15] Thus the trigonal-bipyramidal structure of **1** results from the S linkage in the L^1 ligand, which is folded along the S···Mn line. The fold angle is 60.36(5)°, which is defined as the deviation angle of the pyridine ring with N(3) from the bipyridine plane.

Synthesis and Structures of Nickel(II) Complexes 2 and 3. Treatment of a methanol solution of $NiCl_2 \cdot 6H_2O$ with L^1 in a 1:1 molar ratio gave a green solution, from which $[NiCl(\mu\text{-}Cl)(L^1)]_2$ (**2**) was isolated as green crystals. The structure of **2** was determined by X-ray crystal structure analysis (Figure 2), and selected bond distances and angles are listed in Table 2. Complex **2** has a dimeric structure consisting of two $NiCl_2(L^1)$ units, in which L^1 adopts meridional coordination. The Ni

Table 2. Selected Bond Lengths/Å and Angles/° for **2**

Ni(1)–N(1)	2.0746(18)	Ni(2)–N(4)	2.068(2)
Ni(1)–N(2)	2.066(2)	Ni(2)–N(5)	2.067(2)
Ni(1)–N(3)	2.0996(19)	Ni(2)–N(6)	2.0912(18)
Ni(1)–Cl(1)	2.4254(6)	Ni(2)–Cl(3)	2.4229(6)
Ni(1)–Cl(3)	2.4289(7)	Ni(2)–Cl(1)	2.4162(7)
Ni(1)–Cl(2)	2.4422(7)	Ni(2)–Cl(4)	2.4814(7)
N(1)–Ni(1)–N(2)	79.49(8)	N(4)–Ni(2)–N(5)	79.53(8)
N(2)–Ni(1)–N(3)	92.94(7)	N(5)–Ni(2)–N(6)	93.47(7)
N(1)–Ni(1)–N(3)	168.91(8)	N(4)–Ni(2)–N(6)	169.33(8)
N(2)–Ni(1)–Cl(1)	171.21(6)	N(5)–Ni(2)–Cl(3)	170.98(6)
Cl(1)–Ni(1)–Cl(3)	84.87(2)	Cl(1)–Ni(2)–Cl(3)	85.20(2)
Cl(2)–Ni(1)–Cl(3)	176.75(2)	Cl(1)–Ni(2)–Cl(4)	176.53(2)
Ni(1)–Cl(1)–Ni(2)	95.10(2)	Ni(1)–Cl(3)–Ni(2)	94.83(2)
C(10)–S(1)–C(11)	107.44(11)	C(25)–S(2)–C(26)	108.03(12)

centers are doubly bridged by chloro ligands and the other two chloride ions act as terminal ligands to form two edge-shared N_3Cl_3 octahedra. The dinuclear structure has pseudo C_i symmetry with the inversion center at the midpoint between two Ni atoms. The Ni–N bonds from pyridylthio groups are somewhat longer than those from bipyridine moieties: average, Ni–N(c) = 2.067(2) Å, Ni–N(pyC) = 2.071(2) Å, Ni–N(pyS) = 2.095(2) Å; c, pyC, and pyS in parentheses denote a central donor atom in a tridentate ligand, and terminal pyridyl groups bound to C and S atoms, respectively. The trans angles, N(1)–Ni(1)–N(3) and N(4)–Ni(2)–N(6) in **2** are 168.91(8) and 169.33(8)°, respectively. These structural features are different from those of terpyridine nickel(II) complexes, which usually show significant decreases of the Ni–N(c) bond distance and the N–Ni–N trans angle.[16–18] The meridionally coordinated L^1 ligand in **2** shows deviation from planarity at the S linkage: the fold angles between bipyridine and pyridine units are 36.66(8) and 33.36(8)°. Although these angles are considerably smaller than that in **1** (60.36(5)°), all the Ni–N bonds in **2** are comparable to those in $[Ni(bpy)_3]SO_4$ (average, 2.089(9) Å).[19] Thus, there is no significant strain in the coordination geometry in **2** because of the flexible S linkage in L^1.

The 2:1 reaction of L^1 with $Ni(CH_3COO)_2 \cdot 4H_2O$ afforded purple crystals of $[Ni(L^1)_2](SbF_6)_2$ (**3**) by adding $NaSbF_6$. The crystal structure of **3** is shown in Figure 3, and selected bond distances and angles are given in Table 3. Two L^1 ligands are bound through three N atoms in a meridional fashion. The Ni–N bonds from terminal N atoms in bipyridine units in **3** (Ni–N(1) = 2.124(3) Å, Ni–N(4) = 2.114(3) Å) are slightly longer than the corresponding Ni–N distances in **2** (2.0746(18) and 2.068(2) Å). Furthermore, the fold angles of L^1 (44.61(15) and 47.34(15)°) are larger than those in **2**. These results suggest that the bis-coordination of L^1 in **3** induces the repulsive intramolecular interactions between the terminal and central pyridine rings in different ligands. In contrast, the Ni–N distances of terpyridine complexes are similar between mono- and bis-complexes, which is due to the smaller intraligand N–Ni–N trans angles reducing the steric repulsion between ligands.[16–18,20,21]

Synthesis and Structures of Palladium(II) Complexes 4 and 5. Palladium complexes were synthesized for both L^1 and L^2 ligands. The reaction of L^1 with $Li_2[PdCl_4]$ in methanol gave an orange suspension, from which orange crystals of $[PdCl(L^1)]Cl$ (**4**) were obtained. The corresponding L^2 complex $[PdCl(L^2)]$ (**5**) was synthesized by heating a dimethyl sulfoxide (DMSO) solution of the ligand precursor HL^2 and $Li_2[PdCl_4]$ at 150 °C (Scheme 3). In ^1H NMR experiments (DMSO-d_6), 70% of HL^2 was cyclopalladated to form **5** after heating at 150 °C for 4 h and no other new signals were observed. Thus the C–H bond between 2-pyridyl and 2-pyridylthio groups in HL^2 is selectively activated. The high regioselectivity stems from the two pyridyl groups in HL^2 since precoordination of the pyridyl group was found to facilitate the cyclometallation.[22,23]

The structures of **4** and **5**, which were confirmed by X-ray structure analysis, are shown in Figures 4 and 5, respectively. Selected bond distances and angles are summarized in Table 4. In both complexes, the palladium ion is surrounded by a tridentate ligand and a chloride ion to form a square-planar

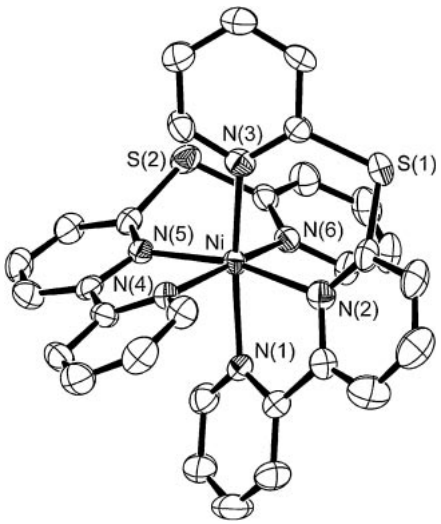

Figure 3. ORTEP drawing of **3** with thermal ellipsoids at the 50% probability level. Hexafluoroantimonate anions and hydrogen atoms are omitted for clarity.

Table 3. Selected Bond Lengths/Å and Angles/° for **3**

Ni–N(1)	2.124(3)	Ni–N(4)	2.114(3)
Ni–N(2)	2.068(3)	Ni–N(5)	2.064(3)
Ni–N(3)	2.092(3)	Ni–N(6)	2.104(3)
N(1)–Ni–N(2)	76.44(14)	N(4)–Ni–N(5)	77.20(13)
N(2)–Ni–N(3)	93.90(14)	N(5)–Ni–N(6)	93.42(14)
N(1)–Ni–N(3)	169.53(14)	N(4)–Ni–N(6)	168.38(14)
N(2)–Ni–N(5)	166.72(15)		
C(10)–S(1)–C(11)	105.9(2)	C(25)–S(2)–C(26)	106.0(2)

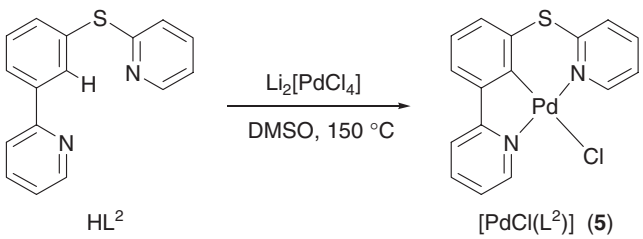

Scheme 3. Synthesis of the palladium complex $[PdCl(L^2)]$ (**5**).

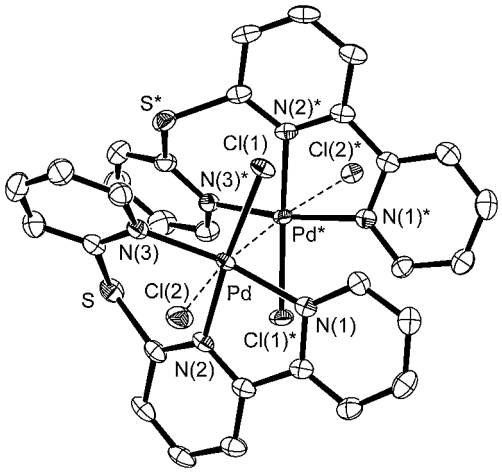

Figure 4. ORTEP drawing of **4** with thermal ellipsoids at the 50% probability level. Hydrogen atoms are omitted for clarity.

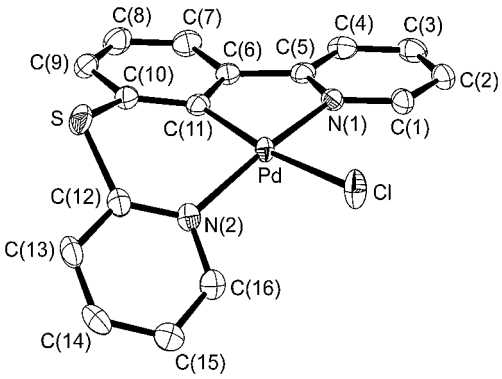

Figure 5. ORTEP drawing of **5** with thermal ellipsoids at the 50% probability level. Hydrogen atoms are omitted for clarity.

complex, $[PdCl(L^1)]^+$ or $[PdCl(L^2)]$. As shown in Figure 4, the complex cations $[PdCl(L^1)]^+$ in **4** tend to pair, forming a face to face dimer with a Pd···Pd distance of 3.5387(2) Å. There is a relatively short contact of 3.5448(7) Å between the counter ion Cl^- and the Pd atom. The Cl(2)···Pd···Pd*···Cl(2)* arrangement is close to linear with a Cl(2)–Pd–Pd* angle of 174.297(11)°, which suggests the weak bonding interactions in the axial direction. In complex **5**, L^2 acts as an anionic *N*,*C*,*N*-tridentate ligand, which forms a five-membered and a six-membered metallacycle (Figure 5). There is no Pd···Pd interaction in the crystal structure of **5**, while π–π stacking interactions are observed between the pyridyl ring containing N(1) and the five-membered chelate ring with C(11) and N(1) donor atoms: N(1)···C(5)*, C(5)···N(1)*, 3.471(2); C(6)···C(1)*, 3.422(2); C(11)···C(2)*, 3.435(2); Pd···C(3)*, 3.753(2); Pd···C(4)*, 3.7204(19) Å. The Pd–C distance in **5** (1.9577(19) Å) is smaller than the Pd–N(central) distance in **4** (2.0069(16) Å), while the Pd–Cl distance in **5** (2.4191(5) Å) is larger than that in **4** (2.2936(4) Å), indicating a strong trans influence of the carbon donor atom in **5**. Other bond distances and angles are similar between **4** and **5**. The fold angles between bipyridine (or phenylpyridine) and pyridine units in **4** and **5** are 45.53(8) and 39.14(6)°, respectively. These values are similar to those of the six-coordinate complexes **2** and **3**, and smaller than that of the five-coordinate complex **1**.

Table 4. Selected Bond Lengths/Å and Angles/° of **4** and **5**

	4	**5**
Pd–N(c) or C(c)[a)]	2.0069(16)	1.9577(19)
Pd–N(pyC)[a)]	2.0108(18)	2.0435(15)
Pd–N(pyS)[a)]	2.0350(18)	2.0655(17)
Pd–Cl	2.2936(4)	2.4191(5)
N(c)–Pd–N(pyC)[a)]	80.83(6)	80.74(7)
N(c)–Pd–N(pyS)[a)]	94.76(6)	93.39(7)
N(pyC)–Pd–N(pyS) or N(pyC)[a)]	167.29(7)	165.69(6)
N(pyC)–Pd–Cl[a)]	94.71(4)	95.64(4)
N(c)–Pd–Cl[a)]	172.01(5)	171.64(5)
N(pyS)–Pd–Cl[a)]	90.95(4)	91.81(5)
C–S–C	105.37(11)	105.47(9)

a) Abbreviations c, pyC, and pyS in parentheses mean a central donor atom in a tridentate ligand, 2-pyridyl groups bound to C and S atoms, respectively.

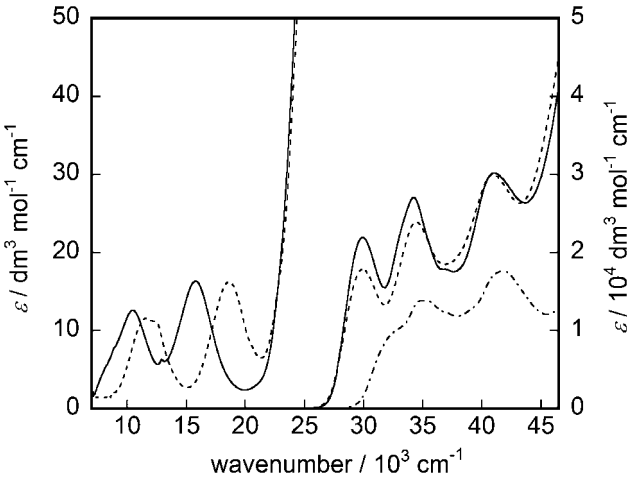

Figure 6. Absorption spectra of **2** in methanol (—), **3** in acetonitrile (- - -), and L^1 in methanol (· · ·).

The coordination geometries of **4** and **5** are compared with those of the analogous palladium(II) complexes, $[PdCl(terpy)]Cl$[24] and $[PdCl(L_{N,C,N})]$,[11] where $L_{N,C,N}$ is a 2,6-bis(2-pyridyl)phenyl ligand. The Pd–N(c) distance in **4** is larger than that in $[PdCl(terpy)]Cl$ (1.96(2) Å) by ca. 0.05 Å. Similar elongation was observed for the Pd–C distance in **5** by comparison with $[PdCl(L_{N,C,N})]$ (1.910(2) Å). The Pd–Cl distances are 2.313(7) Å for $[PdCl(terpy)]Cl$ and 2.427(1) Å for $[PdCl(L_{N,C,N})]$, which are similar to those for **4** and **5**, respectively. Thus the NCN pincer ligands show the elongation of the Pd–Cl bond by ca. 0.1 Å compared with the corresponding NNN tridentate ligands.

Spectroscopic Characterization of Complexes. Absorption spectra of L^1, **2**, and **3** are shown in Figure 6, and spectral data for L^1 and all the complexes are summarized in Table 5. Ligand L^1 exhibits intense bands above 29000 cm^{-1} (below 340 nm), which are assignable to π–π^* transitions (Figure 6). The spectrum of manganese(II) complex **1** was quite similar to that of L^1 in dilute conditions, which suggests the dissociation of the ligand.

Table 5. Absorption Spectral Data for L^1, **1**, **2**, **3**, **4**, and **5**

Complex (solvent)	λ_{max}/nm (ε/mol^{-1} dm^3 cm^{-1})
L^1 (CH_3OH)	315 (8300),[a] 284 (13800), 239 (17600)
1 (CH_3OH)	316 (8100),[a] 283 (13900), 239 (17600)
2 (CH_3OH)	952 (12.6), 773 (6.21), 633 (16.2), 334 (21900), 292 (27000), 244 (30200)
3 (CH_3CN)	870 (11.6), 795 (11.0),[a] 537 (16.2), 335 (17900), 291 (23900), 245 (30000)
4 (CH_3OH)	351 (8300), 303 (9500), 255 (18400),[a] 233 (30000)
5 (DMSO)	373 (2800),[a] 332 (9370), 320 (9390), 275 (20400)

a) Shoulder.

Nickel(II) complexes **2** and **3** show intense bands above 27000 cm^{-1} (below 370 nm), which are assignable to π–π^* transitions localized on the ligand (Figure 6). In the visible region, **2** displays two bands at 10500 (952 nm) and 15800 cm^{-1} (633 nm), which are assignable to d–d transitions, $^3T_{2g}(F) \leftarrow {}^3A_{2g}$ and $^3T_{1g}(F) \leftarrow {}^3A_{2g}$, respectively. The dimeric structure of **2** can be dissociated to the mononuclear species such as $[NiCl_{2-n}(L^1)(CH_3OH)_{1+n}]^{n+}$ ($n = 0$, 1, and 2) in methanol because of the lability of the nickel(II) center. The electrospray ionization (ESI) mass spectrum of **2** in methanol exhibited peaks due to the $[Ni(L^1)(CH_3OH)]^{2+}$ ion. The absorption spectrum of **2** readily changed to that of **3** by adding an equimolar amount of L^1. The $[Ni(L^1)_2]^{2+}$ ion was observed in the ESI mass spectrum of **3**. An acetonitrile solution of **3** showed the absorption bands at 11500 cm^{-1} (870 nm) and 18600 (537 nm), which were assigned to d–d transitions, $^3T_{2g}(F) \leftarrow {}^3A_{2g}$ and $^3T_{1g}(F) \leftarrow {}^3A_{2g}$, respectively, in a symmetry near O_h. The transition energies of these bands are smaller than those of $[Ni(terpy)_2](ClO_4)_2$ in acetonitrile (12600 and 19400 cm^{-1}) and $[Ni(bpy)_3]Cl_2$ in H_2O (12600 and 19300 cm^{-1}).[20,25] The reduction in Δ_O for **3** is related to the six-membered chelate and the intramolecular repulsion of L^1 found in the crystal structure.

The absorption spectrum of palladium(II) complex **4** in methanol was characterized by three intense bands in the range of 220–390 nm. The absorption at 28500 cm^{-1} (351 nm) can be attributed to a metal to ligand charge-transfer (MLCT) transition by analogy to terpyridine palladium(II) complexes.[26] The higher-energy transitions are related to intraligand π–π^* transitions.

The ^{1}H NMR spectrum of **4** showed that the L^1 ligand in **4** partially dissociates in a DMSO-d_6 solution at room temperature (Figure 7). The ratio of **4** and L^1 was 5:1, and the complex cation $[Pd(Me_2SO)_4]^{2+}$ would be formed.[27,28] This dissociation results from the coordination ability of DMSO because no signal of free L^1 was observed in methanol-d_4. In contrast, the L^2 ligand in complex **5** is stable in DMSO as expected from the synthesis conditions. The strong σ-donating character of aryl C donor of L^2, which forms stable metallacycles, prevents the dissociation of L^2 in DMSO. In the NMR spectra of **4** and **5**, two 6-positioned H signals of 2-pyridyl and 2-pyridylthio groups exhibit low field shifts compared with those of the free ligands. This suggests that the 2-pyridylthio group, as well as the 2-pyridyl group, is bound to Pd in the solution.

Mizoroki–Heck Reaction Catalyzed by Palladium(II) Complexes. Catalytic activities of palladium(II) complexes **4** and **5** were investigated for the Mizoroki–Heck reaction of iodobenzene and methyl acrylate. All reactions were performed in *N*,*N*-dimethylformamide (DMF) in the presence of triethylamine as a base. The results are summarized in Table 6. The reactions in Entries 1 and 2 were carried out at 110 °C for 5 h using **4** and **5** as catalysts (0.1 mol %), respectively, and were monitored by ^{1}H NMR spectroscopy. Figure 8 shows the time course of the yields of methyl *trans*-cinnamate. Catalysts **4** and **5** gave excellent conversions after 40 min and 3 h, respectively. The faster rate for the reaction with **4** indicates that the formation of the catalytically active species from **4** is faster than that from **5**. When the reactions were performed at 80 °C for 5 h, catalyst **4** gave a good yield (92%), while **5** reduced the yield to 6% (Entries 3 and 4). Palladium black was precipitated

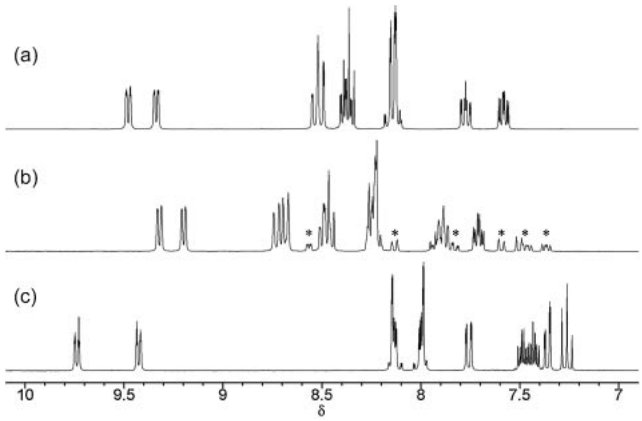

Figure 7. ^{1}H NMR (300 MHz) spectra of (a) **4** in methanol-d_4, (b) **4** in DMSO-d_6, and (c) **5** in DMSO-d_6. Asterisks denote the signals of the free ligand L^1.

Table 6. Mizoroki–Heck Reactions Catalyzed by Palladium Complexes **4** and **5**

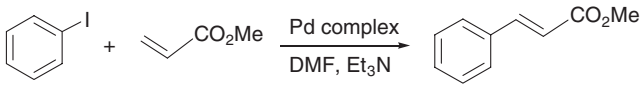

Entry	Catalyst (mol %)	T/°C	Time/h	Yield/%[a]
1	**4** (0.1)	110	5	>99
2	**5** (0.1)	110	5	>99
3	**4** (0.1)	80	5	92
4	**5** (0.1)	80	5	6
5	**4** (0.001)	110	5	7
6	**5** (0.001)	110	5	6
7	**4** (0.001)	110	15	22
8	**5** (0.001)	110	15	20

a) Yields are given relative to iodobenzene.

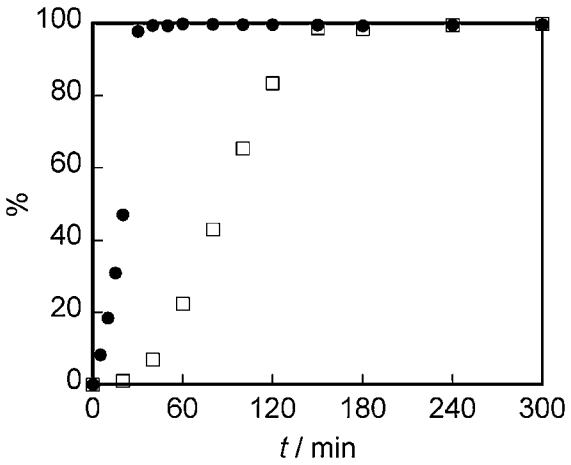

Figure 8. Time course of the yields of methyl *trans*-cinnamate for the Mizoroki–Heck reactions of iodobenzene (2 mmol) and methyl acrylate (3 mmol) catalyzed by **4** (0.1 mol %, ●) and **5** (0.1 mol %, □). The reactions were performed in *N*,*N*-dimethylformamide (10 mL) at 110 °C, using triethylamine (3 mmol) as a base.

only in the reaction of Entry 1 (0.1 mol % of catalyst **4**, 110 °C). This could be related to the solution behavior suggested by the NMR data. Ligand L^1 in **4** can dissociate in the reaction solution, while the coordination of L^2 in **5** remains intact. Reetz and de Vries recently proposed the reaction mechanism catalyzed by ligand-free palladium.[29,30] Although the actual catalytically active species in the reactions studied here remain elusive, the results indicate that the strong σ-donating character of the C donor atom in L^2 prevents the formation of active Pd(0) species from **5**.

Lower catalyst loadings (0.001 mol %) significantly reduced the yield for both **4** and **5**, even when the reaction time was extended to 15 h (Entries 5–8). The turnover frequencies were 1400 h^{-1} for **4** and 1300 h^{-1} for **5**, which are lower than that for the corresponding reactions using [PdCl($L_{N,C,N}$)] (5400 h^{-1}) containing two five-membered palladacycles.[11] An analogous complex with a 2,6-bis(2-pyridyloxy)phenyl ligand has two six-membered palladacycles, and showed higher turnover frequencies under very dilute conditions.[12] Complex **5** has a five- and a six-membered palladacycle. The catalytic activity of the NCN pincer Pd complexes is affected by the electronic effect of the linkage atom, as well as the geometry around the metal center.

Conclusion

The terpyridine-like ligand L^1 containing a sulfur linkage was isolated and used for the manganese(II), nickel(II), and palladium(II) complexes. Five-, six-, and four-coordinate complexes were presented for Mn, Ni, and Pd, respectively. The fold angle between bipyridine and pyridine units varied from 60.36(5) to 33.36(8)°. These values are indicative of flexibility of L^1 in coordination compounds.

The NCN pincer palladium(II) complex **5**, which is geometrically analogous to the L^1–palladium(II) complex **4**, was synthesized via the regioselective C–H activation of the ligand precursor HL^2. The strong σ-donating character of the aryl carbon donor results in the different solution behavior of **5** compared to **4**. The S-linked ligands, L^1 and L^2, would be applicable as tridentate polypyridine ligands for a wide range of transition-metal ions. Further applications of these ligands to transition metal-catalyzed reactions are in progress.

Experimental

Materials and Instrumentation. All reagents were purchased from commercial sources and used as received. 6-Bromo-2,2′-bipyridine was prepared according to literature procedures.[31] Lithium tetrachloropalladate(II) was prepared by refluxing an aqueous solution of $PdCl_2$ (1 equiv) and LiCl (2 equiv) for 2 h. NMR spectra were recorded on a JEOL Lambda 300 or a Bruker AVANCE 300 FT-NMR spectrometer at room temperature. UV–vis spectra were measured on a JASCO V-570 spectrometer. ESI mass spectrometry was performed on an Applied Biosystem Mariner time-of-flight mass spectrometer. Elemental analyses were performed by the Analytical Research Service Center at Osaka City University on Perkin-Elmer 240C or FISONS Instrument EA1108 elemental analyzers.

6-(2″-Pyridylthio)-2,2′-bipyridine (L^1). A suspension of 6-bromo-2,2′-bipyridine (0.71 g, 3.0 mmol) and pyridine-2-thiol (0.50 g, 4.5 mmol) in deoxygenated 1,2-propanediol (15 mL) was stirred at 120 °C for 3 h under an argon atmosphere. To the resulting bright yellow solution were added water (50 mL) and chloroform (30 mL), followed by stirring for 1 h. The organic layer was separated, and then the aqueous layer was extracted with chloroform (30 mL). The combined extract and organic layer were washed with water, dried over Na_2SO_4, filtered, and concentrated to dryness. The residual orange oil was purified by column chromatography (silica gel, 2 cm × 12 cm, *n*-hexane/ethyl acetate, 1:1). Ligand L^1 was obtained as a pale yellow oil (0.65 g, 81%). ^{1}H NMR (300 MHz, $CDCl_3$, Me_4Si): δ 7.20 (ddd, $J = 7.4$, 4.9, 1.2 Hz, 1H, 5″-H), 7.29 (ddd, $J = 7.5$, 4.8, 1.2 Hz, 1H, 5′-H), 7.43 (dd, $J = 7.8$, 0.9 Hz, 1H, 5-H), 7.54 (dt, $J = 8.0$, 1.1 Hz, 1H, 3″-H), 7.65 (ddd, $J = 8.0$, 7.4, 1.9 Hz, 1H, 4″-H), 7.74 (t, $J = 7.8$ Hz, 1H, 4-H), 7.75 (ddd, $J = 8.0$, 7.5, 1.8 Hz, 1H, 4′-H), 8.26 (dt, $J = 8.0$, 1.0 Hz, 1H, 3′-H), 8.27 (dd, $J = 7.8$, 0.9 Hz, 1H, 3-H), 8.59 (ddd, $J = 4.9$, 1.9, 0.9 Hz, 1H, 6″-H), 8.66 (ddd, $J = 4.8$, 1.8, 0.9 Hz, 1H, 6′-H). ^{1}H NMR (300 MHz, DMSO-d_6, Me_4Si): δ 7.36 (ddd, $J = 7.5$, 4.8, 1.0 Hz, 1H), 7.46 (ddd, $J = 7.5$, 4.8, 1.2 Hz, 1H), 7.51 (dd, $J = 7.8$, 0.8 Hz, 1H), 7.59 (dt, $J = 8.0$, 0.9 Hz, 1H), 7.84 (td, $J = 7.7$, 1.9 Hz, 1H), 7.92 (td, $J = 7.7$, 1.8 Hz, 1H), 7.93 (t, $J = 7.8$ Hz, 1H), 8.14 (dt, $J = 7.9$, 0.9 Hz, 1H), 8.27 (dd, $J = 7.8$, 0.8 Hz, 1H), 8.56 (ddd, $J = 4.8$, 1.8, 0.8 Hz, 1H), 8.69 (ddd, $J = 4.8$, 1.8, 0.9 Hz, 1H). ^{13}C NMR (75.5 MHz, $CDCl_3$, Me_4Si): δ 118.8 (3-C), 121.3 (3′-C), 121.9 (5″-C), 123.9 (5′-C), 125.2 (5-C), 126.5 (3″-C), 136.86 (4′-C), 136.94 (4″-C), 137.9 (4-C), 149.1 (6′-C), 150.2 (6″-C), 155.4 (2′-C), 156.4 (2- or 6-C), 156.5 (2- or 6-C), 156.8 (2″-C). HRMS (ESI$^+$): m/z calcd for $^{12}C_{15}{}^1H_{12}{}^{14}N_3{}^{32}S_1$ ([M + H]$^+$): 266.0746. Found: 266.0729.

1-Bromo-3-(2′-pyridylthio)benzene. To a deoxygenated solution of 1,3-dibromobenzene (4.7 g, 20 mmol) and pyridine-2-thiol (3.3 g, 30 mmol) in DMF (80 mL) was added K_2CO_3 (4.1 g, 30 mmol). The reaction mixture was refluxed for 5 h under an argon atmosphere. The resulting pale yellow suspension was filtered and concentrated to dryness. The yellow

residue was purified by column chromatography (silica gel, 2.5 cm × 40 cm, *n*-hexane/ethyl acetate, 1:1) to give a colorless liquid (1.66 g, 31%). ^{1}H NMR (300 MHz, $CDCl_3$, Me_4Si): δ 7.00 (dt, $J = 8.0$, 1.0 Hz, 1H, 3′-H), 7.05 (ddd, $J = 7.5$, 4.9, 1.0 Hz, 1H, 5′-H), 7.28 (t, $J = 7.9$ Hz, 1H, 5-H), 7.48–7.55 (m, 3H, 4-, 6-, and 4′-H), 7.73 (t, $J = 1.8$ Hz, 1H, 2-H), 8.45 (ddd, $J = 4.9$, 1.9, 0.9 Hz, 1H, 6′-H). ^{13}C NMR (75.5 MHz, $CDCl_3$, Me_4Si): δ 120.5, 122.1, 123.1, 130.8, 131.9, 132.9, 133.6, 136.8, 136.9, 149.8, 159.9. HRMS (ESI$^+$): m/z calcd for $^{12}C_{11}{}^1H_9{}^{79}Br_1{}^{14}N_1{}^{32}S_1$ ($[M + H]^+$): 265.9634. Found: 265.9637.

3-(2′-Pyridylthio)phenylboronic Acid. 1-Bromo-3-(2′-pyridylthio)benzene (2.12 g, 8.0 mmol) was dissolved in dry diethyl ether (40 mL) under an argon atmosphere and cooled to −90 °C using a liquid nitrogen/methanol bath. *n*-Butyllithium (1.6 M, 1 M = 1 mol dm^{-3}) in *n*-hexane (5.5 mL, 8.8 mmol) was added dropwise via a syringe, and the mixture was allowed to warm to −40 °C for 40 min. The pale yellow suspension was cooled to −80 °C, and then trimethyl borate (1.8 mL, 16 mmol) was added. The mixture was allowed to warm to room temperature and stirred for 10 h. To the resulting colorless suspension, cooled to 0 °C, was added 2 M aqueous hydrochloric acid (30 mL), and the mixture was stirred at room temperature for 2 h. The aqueous layer was neutralized using K_2CO_3, and extracted with diethyl ether (total 200 mL). The organic layer and extracts were combined, washed with water, dried over Na_2SO_4, filtered, and concentrated to dryness. The colorless residue was taken up in chloroform (30 mL), filtered, washed with chloroform, and dried under reduced pressure to give a white powder. Yield: 1.20 g (65%). ^{1}H NMR (300 MHz, DMSO-d_6, Me_4Si): δ 6.90 (dt, $J = 8.1$, 0.9 Hz, 1H, 3′-H), 7.14 (ddd, $J = 7.4$, 4.8, 0.9 Hz, 1H, 5′-H), 7.47 (t, $J = 7.5$ Hz, 1H, 5-H), 7.60–7.67 (m, 2H, 4- or 6-H), 7.89 (dt, $J = 7.4$, 1.1 Hz, 1H, 4- or 6-H), 8.00 (s, 1H, 2-H), 8.23 (s, br, 2H, BO*H*), 8.40 (ddd, $J = 4.8$, 1.8, 0.8 Hz, 1H, 6′-H). ^{13}C NMR (75.5 MHz, DMSO-d_6, Me_4Si): δ 120.2, 120.7, 129.0, 129.1, 134.9, 136.4, 137.3, 140.4, 149.4, 160.3. Anal. Calcd for $C_{11}H_{10}BNO_2S$: C, 57.17; H, 4.36; N, 6.06%. Found: C, 57.21; H, 4.46; N, 5.85%. HRMS (ESI$^+$): m/z calcd for $^{12}C_{11}{}^1H_{11}{}^{11}B_1{}^{14}N_1{}^{16}O_2{}^{32}S_1$ ($[M + H]^+$): 232.0600. Found: 232.0612.

1-(2′-Pyridyl)-3-(2″-pyridylthio)benzene (HL^2). A solution of K_2CO_3 (0.55 g, 4.0 mmol) and 2-bromopyridine (0.32 g, 2.0 mmol) in 1,2-dimethoxyethane/H_2O (3:1, 40 mL) was deoxygenated by bubbling with argon gas. 3-(2′-Pyridylthio)-phenylboronic acid (0.46 g, 2.0 mmol) and $[Pd(PPh_3)_4]$ (23 mg, 0.020 mmol) were added, and the mixture was refluxed for 6 h under argon. To the resulting yellow solution were added chloroform (15 mL) and water (15 mL), followed by stirring for 1 h. The organic and aqueous layers were separated, and the aqueous layer was extracted with chloroform (15 mL). The combined extract and organic layer were washed with water, dried over Na_2SO_4, filtered, and concentrated to dryness. The residual yellow oil was purified by column chromatography (silica gel, 2 cm × 12 cm, *n*-hexane/ethyl acetate, 1:1). The ligand HL^2 was obtained as a pale yellow solid (0.45 g, 85%). ^{1}H NMR (300 MHz, $CDCl_3$, Me_4Si): δ 6.94 (dt, $J = 8.1$, 0.9 Hz, 1H), 7.00 (ddd, $J = 7.5$, 4.9, 1.0 Hz, 1H), 7.26 (ddd, $J = 6.7$, 4.8, 1.9 Hz, 1H), 7.45 (ddd, $J = 8.1$, 7.5, 1.9 Hz, 1H), 7.54 (t, $J = 7.7$ Hz, 1H), 7.65 (ddd, $J = 7.7$, 1.7, 1.3 Hz, 1H), 7.70–7.80 (m, 2H), 8.07 (ddd, $J = 7.7$, 1.7, 1.2 Hz, 1H), 8.24 (td, $J = 1.7$, 0.4 Hz, 1H), 8.43 (ddd, $J = 4.9$, 1.9, 0.9 Hz, 1H), 8.70 (ddd, $J = 4.8$, 1.7, 1.1 Hz, 1H). ^{13}C NMR (75.5 MHz, $CDCl_3$, Me_4Si): δ 119.9, 120.7, 121.4, 122.6, 127.7, 130.0, 131.7, 133.4, 135.4, 136.8, 136.9, 141.0, 149.6, 149.8, 156.3, 161.4. Anal. Calcd for $C_{16}H_{12}N_2S$: C, 72.70; H, 4.58; N, 10.60%. Found: C, 72.56; H, 4.50; N, 10.42%. HRMS (ESI$^+$): m/z calcd for $^{12}C_{16}{}^1H_{13}{}^{14}N_2{}^{32}S_1$ ($[M + H]^+$): 265.0794. Found: 265.0793.

$[MnCl_2(L^1)]$ (1). A solution of L^1 (67 mg, 0.25 mmol) in ethanol (1 mL) was added to a solution of $MnCl_2 \cdot 4H_2O$ (50 mg, 0.25 mmol) in ethanol (1 mL). The reaction mixture was stirred at room temperature for 30 min. The resulting yellow precipitate was collected by filtration. The product was recrystallized by vapor diffusion of diethyl ether into a methanol solution (12 mL). Yield: 76 mg (77%). Anal. Calcd for $C_{15}H_{11}Cl_2MnN_3S$: C, 46.06; H, 2.83; N, 10.74%. Found: C, 46.35; H, 2.76; N, 10.65%. A piece of crystal was used for single-crystal X-ray structure analysis.

$[NiCl(\mu\text{-}Cl)(L^1)]_2$ (2). A solution of L^1 (67 mg, 0.25 mmol) in methanol (1 mL) was added to a solution of $NiCl_2 \cdot 6H_2O$ (60 mg, 0.25 mmol) in methanol (1 mL). The solution was stirred at room temperature for 30 min to give a green solution. Green crystals were grown by vapor diffusion of diethyl ether into the methanol solution. The crystals were collected by filtration, washed with methanol/diethyl ether (1:1), and air-dried. Pure crystals of **2** were obtained by recrystallization from methanol/diethyl ether. Yield: 70 mg (63%). Anal. Calcd for $C_{30}H_{22}Cl_4N_6Ni_2S_2 \cdot CH_3OH \cdot 3H_2O$: C, 42.51; H, 3.68; N, 9.59%. Found: C, 42.39; H, 3.69; N, 9.76%. MS (ESI$^+$): $m/z = 177.51$ ($[Ni(L^1)(CH_3OH)]^{2+}$). A piece of crystal, the formula of which is $[NiCl(\mu\text{-}Cl)(L^1)]_2 \cdot 3CH_3OH$, was used for single-crystal X-ray structure analysis.

$[Ni(L^1)_2](SbF_6)_2$ (3). To a solution of L^1 (60 mg, 0.23 mmol) in methanol (10 mL) was added $Ni(CH_3COO)_2 \cdot 4H_2O$ (28 mg, 0.11 mmol), and the solution was stirred at room temperature for 30 min. A solution of $NaSbF_6$ (0.11 g, 0.43 mmol) in methanol (2 mL) was added to the reaction solution. After stirring for 30 min, a pink precipitate was collected by filtration. The product was dissolved in DMSO (2 mL) and layered with water. After two weeks purple crystals of **3** were deposited, collected by filtration, washed with water, and air-dried. Yield: 67 mg (56%). Anal. Calcd for $C_{30}H_{22}F_{12}N_6NiS_2Sb_2$: C, 33.96; H, 2.09; N, 7.92%. Found: C, 33.88; H, 2.24; N, 7.90%. MS (ESI$^+$): $m/z = 294.04$ ($[Ni(L^1)_2]^{2+}$). A piece of crystal was used for single-crystal X-ray structure analysis.

$[PdCl(L^1)]Cl$ (4). To a methanol solution (4 mL) of $Li_2[PdCl_4]$ (60 mg, 0.23 mmol) was added L^1 (60 mg, 0.23 mmol) in methanol (4 mL). The resulting orange suspension was stirred at room temperature for 2 days and then filtered. Diethyl ether was diffused into the pale orange filtrate to give pale orange crystals, which were collected by filtration, washed with diethyl ether, and dried under reduced pressure. Yield: 49 mg (47%). ^{1}H NMR (300 MHz, CD_3OD, Me_4Si): δ 7.58 (ddd, $J = 6.7$, 6.0, 2.4 Hz, 1H, 5″-H), 7.77 (ddd, $J = 7.6$, 5.8, 1.4 Hz, 1H, 5′-H), 8.09–8.19 (m, 3H), 8.36 (t, $J = 8.0$ Hz, 1H, 4-H), 8.38 (td, $J = 7.9$, 1.5 Hz, 1H, 4′-H), 8.50 (dd, $J = 8.0$, 1.2 Hz, 1H, 3-H), 8.54 (ddd, $J = 8.2$, 1.4, 0.5 Hz, 1H, 3′-H), 9.34 (ddd, $J = 5.8$, 1.5, 0.5 Hz, 1H, 6′-H), 9.48 (ddd, $J = 6.0$,

Table 7. Crystallographic Data for **1**, **2**, **3**, **4**, and **5**

	1	**2**	**3**	**4**	**5**
Empirical formula	$C_{15}H_{11}Cl_2MnN_3S$	$C_{33}H_{34}Cl_4N_6Ni_2O_3S_2$	$C_{30}H_{22}F_{12}N_6NiS_2Sb_2$	$C_{15}H_{13}Cl_2N_3OPdS$	$C_{16}H_{11}ClN_2PdS$
Formula weight	391.18	886	1060.84	460.65	405.19
Temperature/K	193	113	193	153	153
Wavelength/Å	0.7107	0.7107	0.7107	0.7107	0.7107
Crystal system	monoclinic	monoclinic	orthorhombic	monoclinic	monoclinic
Space group	$P2_1/n$	$P2_1/n$	$Pbca$	$C2/c$	$P2_1/n$
a/Å	7.5467(10)	18.499(5)	14.0794(7)	18.325(3)	9.9901(14)
b/Å	12.2142(17)	9.355(2)	19.2201(8)	15.056(2)	11.3175(14)
c/Å	16.981(2)	21.252(5)	26.1610(11)	12.6184(19)	12.9530(19)
α/°	90	90	90	90	90
β/°	91.804(3)	100.877(3)	90	106.757(3)	106.859(3)
γ/°	90	90	90	90	90
V/Å^3	1564.5(4)	3611.8(16)	7079.4(5)	3333.7(9)	1401.6(3)
Z	4	4	8	8	4
D_{calcd}/Mg m^{-3}	1.661	1.629	1.991	1.835	1.92
μ(Mo Kα)/mm^{-1}	1.315	1.498	2.254	1.565	1.656
F(000)	788	1816	4112	1824	800
Crystal size/mm^3	0.24 × 0.20 × 0.10	0.23 × 0.16 × 0.07	0.31 × 0.09 × 0.06	0.17 × 0.05 × 0.05	0.20 × 0.11 × 0.07
Reflections collected	14262	26344	51670	15286	12287
Independent reflections	3498 (R_{int} = 0.025)	8013 (R_{int} = 0.026)	7970 (R_{int} = 0.030)	3735 (R_{int} = 0.027)	3066 (R_{int} = 0.025)
Completeness to θ	97.5% (θ = 27.48°)	96.9% (θ = 27.48°)	98.3% (θ = 27.48°)	97.6% (θ = 27.48°)	95.4% (θ = 27.48°)
Max. and min. transmission	0.877 and 0.729	0.900 and 0.681	0.873 and 0.628	0.925 and 0.787	0.891 and 0.679
No. of data/restraints/params	3498/0/243	8013/22/473	7970/22/500	3735/11/228	3066/0/234
Goodness of fit on F^2	1.004	1.004	1.004	1.001	1.017
Final R indices [$I > 2\sigma(I)$]	$R1$ = 0.0231	$R1$ = 0.0455	$R1$ = 0.0547	$R1$ = 0.0248	$R1$ = 0.0243
R indices (all data)	$wR2$ = 0.0590	$wR2$ = 0.1779	$wR2$ = 0.2011	$wR2$ = 0.0671	$wR2$ = 0.0678
Largest diff. peak and hole (e Å^{-3})	0.35 and −0.33	1.33 and −1.00	2.51 and −1.32	0.97 and −0.74	0.92 and −0.60

1.4, 0.7 Hz, 1H, 6″-H). ^{13}C NMR (75.5 MHz, CD_3OD, Me_4Si): δ 124.4 (3-C), 125.96 (3′-C), 126.01 (5″-C), 128.5 (5′-C), 129.3 (5-C), 129.5 (3″-C), 142.7 (4″-C), 143.4 (4′-C), 144.1 (4-C), 151.4 (2″-C), 152.1 (2- or 6-C), 153.9 (6′-C), 158.5 (6″-C), 158.8 (2′-C), 160.2 (2- or 6-C). Anal. Calcd for $C_{15}H_{11}Cl_2N_3PdS \cdot H_2O$: C, 39.11; H, 2.84; N, 9.12%. Found: C, 39.15; H, 2.76; N, 8.93%. MS (ESI$^+$): m/z = 407.95 ([Pd(L^1)Cl]$^+$), 387.98 ([Pd(L^1)(OH)]$^+$). A piece of crystal was used for single-crystal X-ray structure analysis.

[PdCl(L^2)] (5). $Li_2[PdCl_4]$ (30 mg, 0.11 mmol) and HL^2 (30 mg, 0.11 mmol) were dissolved in DMSO (3 mL). The brown solution was heated at 150 °C for 14 h. The resulting bright yellow solution, cooled to room temperature, was filtered. The filtrate was layered with water (5 mL) and allowed to stand at room temperature for 3 days. Pale yellow crystals of **5** were deposited, collected by filtration, washed with water, and air-dried. Yield: 25 mg (54%). ^{1}H NMR (300 MHz, DMSO-d_6, Me_4Si): δ 7.26 (t, J = 7.6 Hz, 1H, 5-H), 7.36 (dd, J = 7.7, 1.3 Hz, 1H, 4-H), 7.43 (td, J = 5.9, 3.1 Hz, 1H, 5″-H), 7.48 (td, J = 5.8, 3.1 Hz, 1H, 5′-H), 7.76 (dd, J = 7.6, 1.3 Hz, 1H, 6-H), 7.96–8.04 (m, 2H, 3″- and 4″-H), 8.09–8.17 (m, 2H, 3′- and 4′-H), 9.43 (m, 1H, 6′-H), 9.74 (m, 1H, 6″-H). ^{13}C NMR (75.5 MHz, DMSO-d_6, Me_4Si): δ 119.9 (3′-C), 121.6 (5″-C), 123.2 (6-C), 123.4 (5′-C), 125.3 (3″-C), 126.13 (4- or 5-C), 126.17 (4- or 5-C), 128.9 (1- or 3-C), 139.0 (4″-C), 140.2 (4′-C), 146.5 (1- or 3-C), 151.9 (6′-C), 152.8 (C-Pd), 153.4 (2″-C), 156.6 (6″-C), 164.2 (2′-C). Anal. Calcd for $C_{16}H_{11}ClN_2PdS$: C, 47.43; H, 2.74; N, 6.91%. Found: C, 47.30; H, 2.67; N, 6.70%. A piece of crystal was used for single-crystal X-ray structure analysis.

General Procedure of Mizoroki–Heck Reaction. Iodobenzene (408 mg, 2.0 mmol), methyl acrylate (258 mg, 3.0 mmol), triethylamine (304 mg, 3.0 mmol), and mesitylene (240 mg, 2.0 mmol) as an internal standard were dissolved in DMF (10 mL) containing an appropriate amount of the isolated complex **4** or **5**. The solution was heated at 110 °C for 5 h. To determine the yield of methyl *trans*-cinnamate, 0.05 mL of the reaction solution was used for the ^{1}H NMR measurements in $CDCl_3$. The ^{1}H NMR spectrum of methyl *trans*-cinnamate was identical to that of an authentic sample.

X-ray Crystal Structure Determination of 1, 2, 3, 4, and 5. A single crystal of **1**, **2**, **3**, **4**, or **5** was mounted on a glass fiber. The diffraction data were collected on an AFC7/CCD Mercury diffractometer using the rotation method with 0.5° frame width and with 10 s exposure time per frame. The data were processed and corrected for Lorentz and polarization effects using CrystalClear software.[32] The analyses were carried out using the CrystalStructure 3.8 crystallographic software package.[33] Absorption corrections were applied using the Multi Scan method. The structures were solved using direct methods (SIR97[34]) and refined by full-matrix least-squares on F^2 using CRYSTALS.[35] Crystallographic data are summarized in Table 7. All non-hydrogen atoms were refined anisotropically. Hydrogen atoms in **1** and **5** were found in difference Fourier maps and refined isotropically. Hydrogen atoms in **2**, **3**, and **4** were located on calculated positions and refined as the riding model.

Crystallographic data have been deposited with Cambridge Crystallographic Data Centre: Deposition numbers CCDC-750358, -750359, -750360, -750361, and -750362 for com-

pounds **1**, **2**, **3**, **4**, and **5**, respectively. Copies of the data can be obtained free of charge via http://www.ccdc.cam.ac.uk/conts/retrieving.html (or from the Cambridge Crystallographic Data Centre, 12, Union Road, Cambridge, CB2 1EZ, U.K.; Fax: +44 1223 336033; e-mail: deposit@ccdc.cam.ac.uk).

This work was supported by a Grant-in-Aid for Scientific Research (No. 18350033) from the Ministry of Education, Culture, Sports, Science and Technology of Japan.

References

1 U. S. Schubert, H. Hofmeier, G. R. Newkome, *Modern Terpyridine Chemistry*, WILEY-VCH, Weinheim, **2006**.
2 I. Eryazici, C. N. Moorefield, G. R. Newkome, *Chem. Rev.* **2008**, *108*, 1834.
3 J.-P. Sauvage, J.-P. Collin, J.-C. Chambron, S. Guillerez, C. Coudret, V. Balzani, F. Barigelletti, L. De Cola, L. Flamigni, *Chem. Rev.* **1994**, *94*, 993.
4 S.-W. Lai, M. C. W. Chan, K.-K. Cheung, C.-M. Che, *Inorg. Chem.* **1999**, *38*, 4262.
5 E. Baranoff, J.-P. Collin, L. Flamigni, J.-P. Sauvage, *Chem. Soc. Rev.* **2004**, *33*, 147.
6 J. Limburg, J. S. Vrettos, L. M. Liable-Sands, A. L. Rheingold, R. H. Crabtree, G. W. Brudvig, *Science* **1999**, *283*, 1524.
7 T. J. Anderson, G. D. Jones, D. A. Vicic, *J. Am. Chem. Soc.* **2004**, *126*, 8100.
8 G. D. Jones, C. McFarland, T. J. Anderson, D. A. Vicic, *Chem. Commun.* **2005**, 4211.
9 H.-L. Kwong, W.-S. Lee, *Tetrahedron: Asymmetry* **2000**, *11*, 2299.
10 G. Chelucci, A. Saba, D. Vignola, C. Solinas, *Tetrahedron* **2001**, *57*, 1099.
11 B. Soro, S. Stoccoro, G. Minghetti, A. Zucca, M. A. Cinellu, S. Gladiali, M. Manassero, M. Sansoni, *Organometallics* **2005**, *24*, 53.
12 M. S. Yoon, D. Ryu, J. Kim, K. H. Ahn, *Organometallics* **2006**, *25*, 2409.
13 A. W. Addison, T. N. Rao, J. Reedijk, J. van Rijn, G. C. Verschoor, *J. Chem. Soc., Dalton Trans.* **1984**, 1349.
14 T. Konno, K. Tokuda, J. Sakurai, K. Okamoto, *Bull. Chem. Soc. Jpn.* **2000**, *73*, 2767.
15 C. Mantel, C. Baffert, I. Romero, A. Deronzier, J. Pécaut, M.-N. Collomb, C. Duboc, *Inorg. Chem.* **2004**, *43*, 6455.
16 R. Cortés, M. I. Arriortua, T. Rojo, X. Solans, C. Miravitlles, D. Beltran, *Acta Crystallogr., Sect. C* **1985**, *41*, 1733.
17 T. Rojo, R. Cortés, L. Lezama, M. I. Arriortua, K. Urtiaga, G. Villeneuve, *J. Chem. Soc., Dalton Trans.* **1991**, 1779.
18 M. G. Barandika, R. Cortés, L. Lezama, M. K. Urtiaga, M. I. Arriortua, T. Rojo, *J. Chem. Soc., Dalton Trans.* **1999**, 2971.
19 A. Wada, N. Sakabe, J. Tanaka, *Acta Crystallogr., Sect. B* **1976**, *32*, 1121.
20 A. T. Baker, D. C. Craig, A. D. Rae, *Aust. J. Chem.* **1995**, *48*, 1373.
21 J. McMurtrie, I. Dance, *CrystEngComm* **2005**, *7*, 216.
22 M. Albrecht, G. van Koten, *Angew. Chem., Int. Ed.* **2001**, *40*, 3750.
23 M. Shibue, M. Hirotsu, T. Nishioka, I. Kinoshita, *Organometallics* **2008**, *27*, 4475.
24 G. M. Intille, C. E. Pfluger, W. A. Baker, Jr., *J. Cryst. Mol. Struct.* **1973**, *3*, 47.
25 H. Ito, *Nippon Kagaku Zasshi* **1956**, *77*, 1399.
26 W. Zhang, C. Bensimon, R. J. Crutchley, *Inorg. Chem.* **1993**, *32*, 5808.
27 B. B. Wayland, R. F. Schramm, *Chem. Commun.* **1968**, 1465.
28 B. F. G. Johnson, J. Puga, P. R. Raithby, *Acta Crystallogr., Sect. B* **1981**, *37*, 953.
29 M. T. Reetz, J. G. de Vries, *Chem. Commun.* **2004**, 1559.
30 J. G. de Vries, *Dalton Trans.* **2006**, 421.
31 Y.-Q. Fang, G. S. Hanan, *Synlett* **2003**, 852.
32 *CrystalClear*, Rigaku Corporation, **1999**.
33 *CrystalStructure 3.8*, Crystal Structure Analysis Package, Rigaku and Rigaku/MSC, **2000–2006**.
34 A. Altomare, M. C. Burla, M. Camalli, G. L. Cascarano, C. Giacovazzo, A. Guagliardi, A. G. G. Moliterni, G. Polidori, R. Spagna, *J. Appl. Cryst.* **1999**, *32*, 115.
35 J. R. Carruthers, J. S. Rollett, P. W. Betteridge, D. Kinna, L. Pearce, A. Larsen, E. Gabe, *CRYSTALS*, Chemical Crystallography Laboratory, Oxford, UK, **1999**.